Article

biomaterials applications

Journal of Biomaterials Applications
2014, Vol. 28(8) 1213–1225

DOI: 10.1177/0885328213502100
jba.sagepub.com
SAGE

Gelatin-apatite bone mimetic co-precipitates incorporated within biopolymer matrix to improve mechanical and biological properties useful for hard tissue repair

Jong-Eun Won[1,2], Ahmed El-Fiqi[1,2], Seung-Hwan Jegal[1,2], Cheol-Min Han[1,4], Eun-Jung Lee[1,2], Jonathan C Knowles[2,3] and Hae-Won Kim[1,2,4]

Abstract

Synthetic biopolymers are commonly used for the repair and regeneration of damaged tissues. Specifically targeting bone, the composite approach of utilizing inorganic components is considered promising in terms of improving mechanical and biological properties. We developed gelatin-apatite co-precipitates which mimic the native bone matrix composition within poly(lactide-*co*-caprolactone) (PLCL). Ionic reaction of calcium and phosphate with gelatin molecules enabled the co-precipitate formation of gelatin-apatite nanocrystals at varying ratios. The gelatin-apatite precipitates formed were carbonated apatite in nature, and were homogeneously distributed within the gelatin matrix. The incorporation of gelatin-apatite significantly improved the mechanical properties, including tensile strength, elastic modulus and elongation at break, and the improvement was more pronounced as the apatite content increased. Of note, the tensile strength increased to as high as 45 MPa (a four-fold increase vs. PLCL), the elastic modulus was increased up to 1500 MPa (a five-fold increase vs. PLCL), and the elongation rate was ~240% (twice vs. PLCL). These results support the strengthening role of the gelatin-apatite precipitates within PLCL. The gelatin-apatite addition considerably enhanced the water affinity and the acellular mineral-forming ability in vitro in simulated body fluid; moreover, it stimulated cell proliferation and osteogenic differentiation. Taken together, the GAp-PLCL nanocomposite composition is considered to have excellent mechanical and biological properties, which hold great potential for use as bone regenerative matrices.

Keywords

Composite materials, bone mimetic, bioactive ceramics, polymer matrix, mechanical properties, bone regeneration

Introduction

For the regeneration of hard tissues, including bone and tooth, recent research has focused on the composite approach of combining polymeric matrices with inorganic components.[1–4] Bone matrix is itself a nanocomposite material, composed primarily of collagenous protein in fibrillar form and apatite inorganic nanocrystallites embedded in the protein molecules. Therefore, the use of composite materials in regenerative therapies is an appropriate way of mimicking the native extracellular matrix (ECM) structure of hard tissues.[5–7]

Studies have shown that nanocomposite biomaterials induced better bone cell responses in vitro, and improved bone formation in vivo, as compared to the effects of individual polymeric components.[8–13] Specifically, porous scaffolds made of apatite-precipitated gelatin showed significantly enhanced bone cell responses due to the presence of an osteoconductive

[1]Institute of Tissue Regeneration Engineering (ITREN), Dankook University, Cheonan, South Korea
[2]Department of Nanobiomedical Science & WCU Research Center, Dankook University, Cheonan, South Korea
[3]Biomaterials and Tissue Engineering, University College London Eastman Dental Institute, London, UK
[4]Department of Biomaterials Science, School of Dentistry, Dankook University, Cheonan, South Korea

The first three authors contributed equally to this work.

Corresponding author:
Hae-Won Kim, Dankook University, Shibu, Cheonan 330-714, South Korea.
Email: kimhw@dku.edu

apatite nanocrystalline phase.[14] Bioactive glass, as an inorganic component that can be incorporated into degradable polymers, has also been shown to stimulate bone bioactivity and osteogenic differentiation of progenitor and stem cells, where the ions comprising the bioactive glass were considered to play significant roles.[11,15,16] Moreover, synthetic polymers filled with calcium compounds (phosphates and carbonates) have shown better resistance to biodegradation and the associated catastrophic failure, via an ionic buffering effect on the acidic environments incurred by the polymer degradation.[12,17] From a mechanical perspective, inorganic components, and particularly those formulated at the nanoscale, have been shown to strengthen and stiffen otherwise flexible and weak polymer matrix components.[17–22]

Here we aimed to develop polymer-inorganic nanocomposites with mechanical and biological properties appropriate for bone regeneration. First, we focused on the co-precipitated form of apatite with gelatin, where the apatite nanocrystallites were formed in the gelatin solution; specifically, the calcium and phosphate ionic precursors were co-precipitated with gelatin molecules. A co-precipitation reaction under adjusted conditions is believed to produce a gelatin-apatite (GAp) nanocomponent which closely mimics native bone ECM composition.[23] Next we utilized the GAp co-precipitates for the formulation of a synthetic composite biopolymer. Poly(lactide-*co*-caprolactone) (PLCL) was chosen as the polymer matrix, as it is known to have beneficial properties derived from both poly(lactide) and poly(caprolactone), such as high flexibility and an appropriate rate of degradability, thus resulting in its application to many tissue engineering matrices.[24,25]

The GAp co-precipitates were incorporated into PLCL matrix at differing ratios, and the effects of the GAp addition on the physico-chemical properties, including hydrophilicity and apatite forming ability, were investigated. Changes in mechanical properties, including strength, stiffness and elongation behaviors, were also systematically examined. Furthermore, the cell responses to the GAp-PLCL nanocomposites were addressed in terms of cell proliferation and osteogenic differentiation.

Materials and methods

Production of GAp precipitates and nanocomposites with PLCL

GAp nanocomposite precipitates with different apatite/gelatin ratios (70:30, 50:50 and 30:70 by weight) were prepared by a precipitation reaction, in which calcium nitrate, $Ca(NO_3)_2\ 4H_2O$, and ammonium hydrogen phosphate, $(NH_3)_2HPO_4$, were reacted simultaneously within the gelatin aqueous solution (Type B, bovine skin, Sigma Aldrich), as described previously.[13,14,23] Briefly, two separate solutions of calcium-containing gelatin (Ca-gelatin) and phosphate-containing gelatin (P-gelatin) were mixed at a ratio of [Ca]/[P] equal to 1.67, with vigorous stirring at 40°C and a constant pH 10, which was maintained using NH_4OH solution (28% NH_3 in H_2O, Sigma-Aldrich). The apatite-precipitated gelatin solutions were frozen at −20°C and were then freeze-dried at −80°C. The dried precipitates were washed thoroughly with distilled water and ethanol to remove any byproducts and were finally frozen and freeze-dried. The lyophilized GAp precipitates were then dispersed in trifluoroethanol (TFE) at 15 w/v% with ultrasonic vibration for a few minutes, after which the solution was stirred vigorously for 24 h. Next, PLCL (Boehringer Ingelheim) dissolved in TFE at 15 wt% was mixed with the GAp solution at varying ratios (GAp:PLCL = 1:1, 1:2, 1:4, 1:6 and 1:8) and the solutions were homogenized with vigorous stirring. The compositions and mixing ratios of each component in GAp-PLCL nanocomposites are summarized in Table 1. A thin membrane form was prepared through a phase separation process by casting the homogenized GAp-PLCL solution in a Teflon mold and allowing the solvent to evaporate completely by vacuum drying.

Characterization

The nanocomposite morphology and the distribution of the apatite nanocrystals within the gelatin matrix were observed using a high-resolution transmission electron microscope, HR-TEM (JEM-3010, JEOL, Japan). The chemical bond structure of the nanocomposites was analyzed by Attenuated total reflectance – Fourier transform Infrared spectroscopy (ATR-FTIR) method, using a Varian 640-IR spectrometer. IR spectra were recorded in the range of 4000–400 cm^{-1} at a resolution of 4 cm^{-1}, using GladiATR diamond crystal accessory (PIKE Technologies). The water affinity of the samples was then examined by measuring the water contact angle (Phoenix 300). Data were recorded as the ascending angle after 30 s of applying a water drop, and five samples were tested for each composition.

The in vitro hydroxyapatite (HA) forming ability of the nanocomposites was tested in simulated body fluid (SBF) solution. Each sample was formed as a disc

Table 1. Compositions of the gelatin-apatite (GAp) and its nanocomposites with PLCL used in this study.

Ratio of each constituent	Apatite:Gelatin	30:70, 50:50, 70:30
	GAp:PLCL	1:1, 1:2, 1:4, 1:6, 1:8

shape (15 mm diameter) and was immersed in 10 ml SBF for different time intervals up to 14 days. The HA formation on the surface was investigated by a thin-film mode of X-ray diffraction (XRD). The XRD spectra were collected using Ultima IV Rigaku with CuKα radiation ($\lambda = 1.5418$ Å), generated at 40 mA and 40 kV. Data were acquired in the diffraction angle (2θ) ranging from 4° to 70° with a step size of 0.02° and a scanning speed of 2°/min. FT-IR analysis was also conducted to examine the change in chemical bond structure of the mineralized surface.

Tensile mechanical tests

The tensile mechanical properties of the nanocomposite were measured using an Instron 3344. Samples with different compositions were prepared with a thickness of ~150–200 µm and were then cut to a size of 30 mm × 4 mm with a gauge length of 10 mm. The thickness of each sample was determined from the average value observed on the SEM images, and a total of five samples were tested for each group. Stress–strain curves of each sample were recorded under the application of a static tensile load. Based on the stress–strain curves, the main mechanical parameters, including tensile strength, elastic modulus and elongation rate, were determined. The tensile strength was determined as the highest stress prior to a failure. The elastic modulus was calculated from the slope of the initial elastic linear region. The elongation % was determined as the strain at failure. A total of five samples were tested for each group and the data were averaged.

In vitro osteoblastic responses

The in vitro cell compatibility of the nanocomposites was evaluated in terms of adhesion and proliferation of the pre-osteoblastic (MC3T3-E1; ATCC) cells; moreover, their osteogenic differentiation was determined by alkaline phosphatase (ALP) activity. Cells were sub-cultured in normal growth medium, which consisted of alpha-minimal essential medium (MEM), supplemented with 10% fetal bovine serum (FBS), 2 mM L-glutamine, 50 IU/ml penicillin and 50 µg/ml streptomycin. Samples for the cell tests were prepared as discs (9 mm diameter) and were then sterilized in ethylene oxide. Each sample was placed in each well of 48-well plates, and cells were seeded on each sample at a density of 2×10^3 cells/ml. After culturing for up to seven days, the cell proliferation level was assessed by a cell counting kit (CCK; Dojindo).

To determine the ALP activity of cells, cells were cultured on each sample for 7, 10 and 14 days, and the ALP enzymatic activity was assessed using ALP activity kit (Sigma), as described previously.[13] The double-stranded DNA (dsDNA) quantification was performed using the PicoGreen assay and total protein quantification was assessed by the micro-BCA method, both of which were used to normalize the ALP activity with respect to either total DNA content or total protein content. The cell tests were performed on three replicate samples ($n = 3$) for each condition, and groups were compared by analysis of variance (ANOVA). A p value of <0.05 and <0.01 was considered statistically significant.

Results and discussion

Gelatin-apatite co-precipitates and properties

The GAp mixture solutions co-precipitated at 40°C and pH 10 were filtered and dried, and the co-precipitates were then heat-treated up to 800°C using TGA to observe the weight loss of the organic phase (gelatin) during thermal treatment. As shown in Figure 1, the weight loss of pure apatite precipitate was minimal (less than 1%), while the weight of pure gelatin was determined to substantially decrease with increasing temperature and a complete decomposition at ~550°C. In the GAp co-precipitates, the weight loss pattern was similar to that observed in pure gelatin. The total weight loss increased as apatite content in the GAp decreased; total weight loss measured from the TGA data was about 24%, 37% and 51%, respectively in the co-precipitates of 30%, 50% and 70% gelatin. Results suggested that the gelatin contents in the co-precipitates were lower than those initially intended. It is assumed that some gelatin might be washed out during the filtering process as the gelatin itself is water-soluble. The gelatin losses determined for the

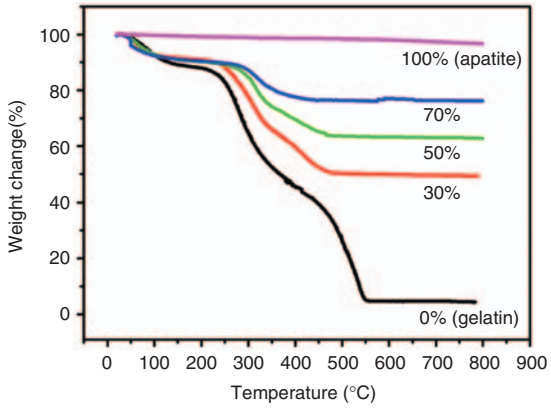

Figure 1. TGA analysis of the GAp co-precipitates synthesized at 40°C and pH 10, presented as the weight change (loss) with respect to a temperature increase up to 800°C. Data on pure gelatin and apatite precipitate were also included for comparison purposes.

experimental materials were about 6%, 13% and 19% for the 30%, 50% and 70% gelatin additions (summarized in Table 2). For convenience, we used the theoretical values as labels throughout this study.

The crystalline phase of the GAp co-precipitates was observed by XRD. As shown in Figure 2(a), well developed crystalline peaks which correspond to the HA were seen for all the GAp compositions. There were no other peaks except for those of HA, suggesting that the co-precipitation reaction was effective in producing a pure apatite phase within the gelatin network. It has been concluded that a collection of amino acids present in gelatin chains are responsible for the nucleation and growth of apatite crystallites[26,27] particularly under the basic conditions used herein (pH 10). In fact, we observed that the apatite phase was not well developed when the pH was neutral (pH 7).

The chemical bonding status of the GAp co-precipitates was analyzed by FT-IR (Figure 2(b)). Data on pure gelatin and apatite precipitate were also shown for comparison purposes. IR bands related to apatite (phosphate modes at 1000–1100 and 560–610 cm^{-1}) were apparent, and the peak intensities increased gradually with increasing apatite content.

The morphology of the GAp co-precipitates was observed by TEM after freeze-drying the filtered co-precipitates, as shown in Figure 3. Co-precipitate sample of 70% apatite was shown as the representative example. Highly elongated apatite nanocrystallites, with sizes of approximately 30 nm × 100 nm, were observed to be embedded within the gelatin matrix. Inset images show the solution of the GAp co-precipitates in TFE, which confirmed the stable micro-emulsion status of the co-precipitates. This stable solution property of the GAp co-precipitates in TFE enabled the formation of a homogeneous mixture of the nanocrystallites with the PLCL polymer, and consequently, the production of nanocomposite samples with evenly distributed apatite nanocrystallites in the PLCL matrix.

Table 2. Summary of the compositions of GAp co-precipitates.

Composition	Gelatin – 30% apatite	Gelatin – 50% apatite	Gelatin – 70% apatite
Theoretical gelatin amount (%)	70%	50%	30%
Experimental gelatin amount (%)	51%	37%	24%
Gelatin deficiency (%)	19%	13%	6%

Theoretical values (intended) applied to the co-precipitation process whilst the experimental ones were calculated from TGA data. The discrepancy noticed between the theoretical and experimental values was due to the loss of gelatin during the process. Gelatin deficiency was 19%, 13% and 6%, respectively in 30%, 50% and 70% apatite.

GAp-PLCL nanocomposites: morphology and water affinity

The GAp co-precipitates were further combined with degradable polymer PLCL to produce nanocomposites. The GAp-PLCL composite solution was cast into a mold to produce a thin membrane, with a thickness of about 150–200 μm. The GAp/PLCL ratios were varied over a wide range, from 1:1 to 1:8. The surface morphology of the nanocomposites was observed by SEM, as shown in Figure 4. Images of some representative compositions (GAp/PLCL 1:1 and 1:6, where apatite contents in gelatin was 70%) are presented. When the GAp content was high (1:1 ratio), some aggregated particles, a few micrometers in size

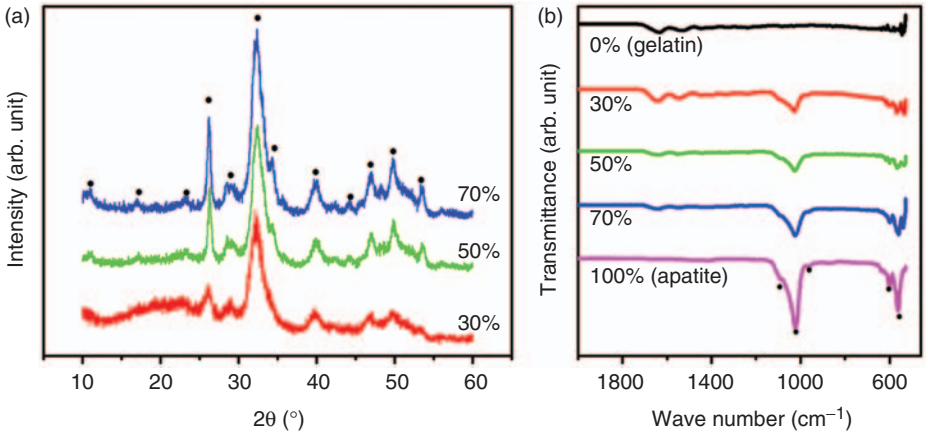

Figure 2. (a) XRD crystalline patterns of the GAp co-precipitates. All peaks developed are related to hydroxyapatite (HA) from JCPDS #74-0566.[32,33] (b) FT-IR analysis of the GAp co-precipitates. Data on pure gelatin and apatite precipitates were also shown for comparison purposes. IR bands related to apatite (phosphate bands at 1000–1100 and 560–610 cm^{-1}) were well noticed with gradual increases in intensity as the apatite content increased.

(arrowed), presumably those of GAp co-precipitates, were seen on the surface (Figure 4(a)), as well as inside the sample (Figure 4(b)). When the GAp content was low (1:6 ratio), the nanocomposite showed a very smooth internal morphology throughout the sample (Figure 4(c)), and the GAP co-precipitates were not readily noticed as they were evenly distributed within the PLCL matrix without being agglomerated, which was different from the sample containing high GAp content. These morphological features of the GAp-PLCL composites should greatly affect the properties such as mechanical strength, and will be discussed in the following section.

The water contact angles of the GAp-PLCL nanocomposites with different compositions were measured, as shown in Figure 5. After dropping distilled water on the surface of the nanocomposites, the ascending angle was measured after 30 s. As the GAp content increased the water contact angle decreased; the contact angle of ~80° in pure PLCL was reduced to ~70° in GAp/PLCL 1:8, and further reduced to ~50° in GAp/PLCL 1:1, demonstrating that the GAp greatly enhanced the hydrophilicity of the nanocomposites. Moreover, this effect was more notable as the gelatin content in GAp was higher. The enhanced hydrophilicity of the nanocomposites driven by the GAp composition is considered to favor their biomedical use in terms of speeding up initial biological events.

Mechanical properties of GAp-PLCL nanocomposites

The mechanical properties of the GAp-PLCL nanocomposites were assessed to determine their feasibility for bone regeneration application. The stress–strain curves of the nanocomposites with different compositions were recorded while applying a static tensile load, and the representative curves of each composition are shown in Figure 6. The result for pure PLCL, as presented for the purpose of comparison, showed a typical stress–strain curve, with a yield point at ~12 MPa, followed by a long elongation and a failure. Because of the broad variation in mechanical strength, which was dependent on the composition, the scales on the *y*-axis were presented differently. Compared to pure PLCL, the nanocomposites resisted higher stresses prior to a yield point. In particular, remarkable improvements were seen with low contents of GAp (GAp/PLCL 1:6 and 1:4), and the improvement was more pronounced when the apatite content in GAp co-precipitates was higher (70% > 50% > 30% apatite).

Based on the stress–strain curves, the tensile strength of the samples was determined as the maximum stress recorded prior to a failure, as presented in Figure 7. Pure PLCL showed an average tensile strength of ~12 MPa. The nanocomposite with the lowest content of GAp (GAp/PLCL 1:8) showed slightly increased strength of ~16 MPa (but only noticed in 70% apatite). When the amount of GAp was further increased (GAp/PLCL 1:6) the strength enhancement of the nanocomposites was

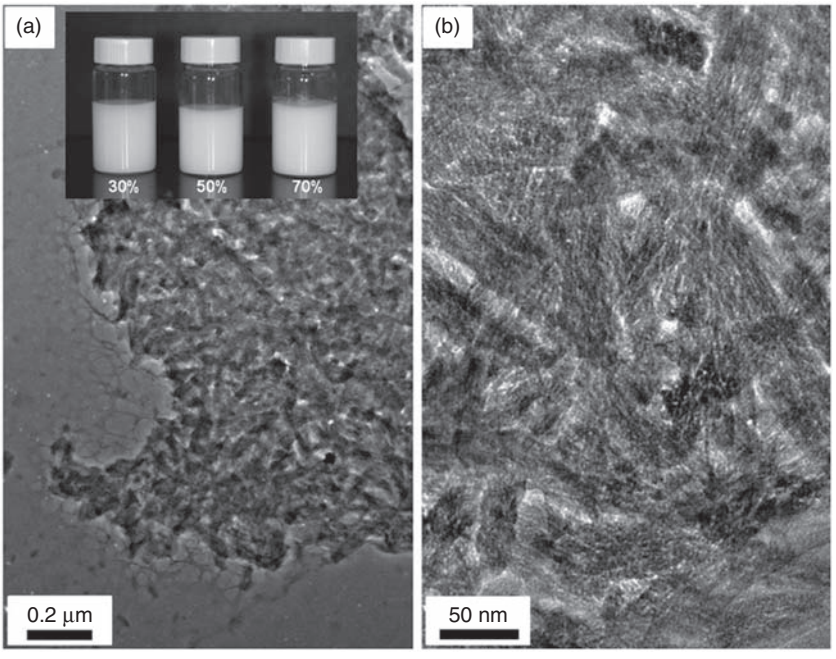

Figure 3. TEM morphology of the GAp co-precipitates, after they were filtered from a co-precipitate solution and then freeze-dried; (a) low and (b) high magnification. Inset in (a) is the solution of GAp co-precipitates (30%, 50% and 70% apatite), showing a stable microemulsion state, which enables a homoftabeneous mixture of GAp co-precipitates within the PLCL polymer.

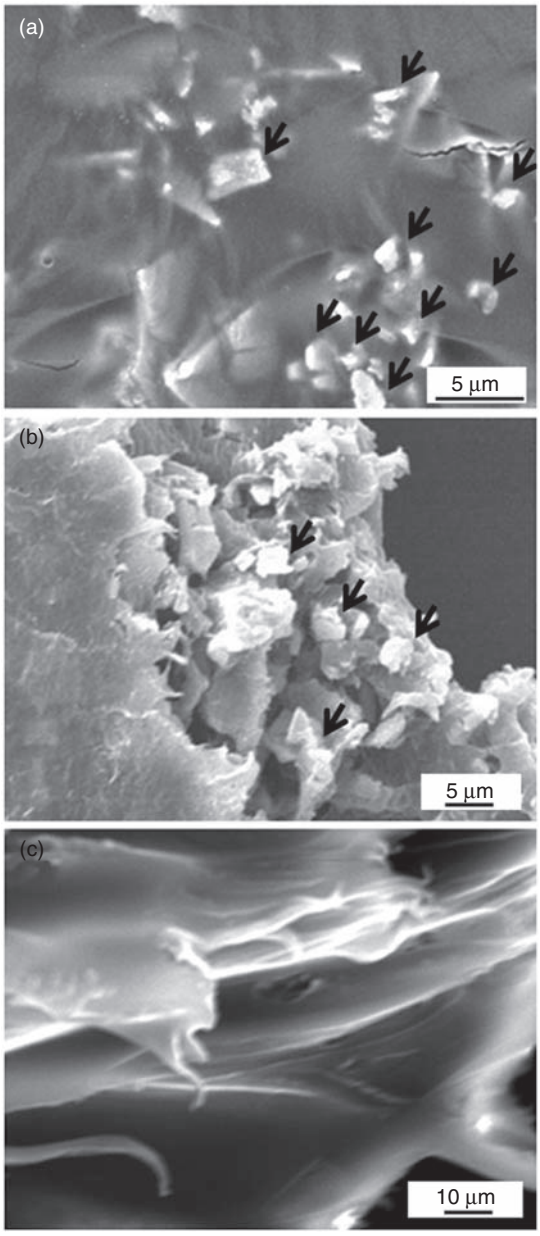

Figure 4. SEM morphology of the nanocomposites of GAp co-precipitates and PLCL; (a, b) GAp/PLCL 1:1 and (c) GAp/PLCL 1:6. Arrows in (a, b) indicate agglomerates of GAp co-precipitates within the PLCL matrix, illustrating the poor dispersion of GAp components when added at a high content; however, no agglomerates were observed when the GAp was added at a lower content (c).

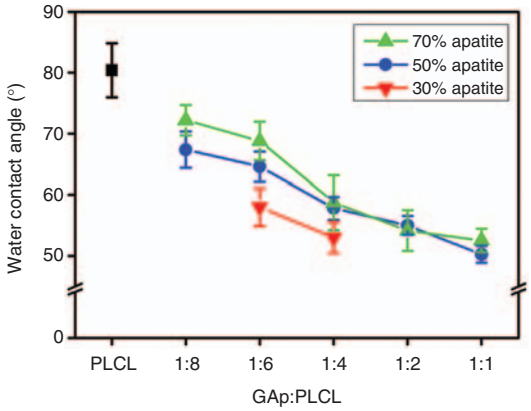

Figure 5. Water contact angle measured on the GAp-PLCL nanocomposites, as presented with respect to varying compositions (GAp/PLCL ratio and apatite content in GAp). Tests were carried out on the surface of the nanocomposites after dropping distilled water and measuring the ascending angle after 30 s. As the GAp content increased, the contact angle decreased, demonstrating that the GAp greatly enhanced the hydrophilicity of the nanocomposite. This effect appeared to be more noticeable in the higher gelatin content (i.e. lower apatite content) in GAp co-precipitates. The contact angle of ~80° decreased down to ~50° at GAp-PLCL 1:1.

tremendous; ~21 MPa, 32 MPa and 45 MPa, respectively for 30%, 50% and 70% apatite, showing an ongoing increase in strength with increasing the apatite content. In the nanocomposite of GAp/PLCL 1:4, such a dramatic strength increase was also noticed, but this was only in the 70% apatite (~40 MPa). However, with further increases of the GAp content (GAp/PLCL 1:2 and 1:1) the strengths were reduced to levels comparable to that of pure PLCL.

It was clearly demonstrated that the GAp co-precipitates, and particularly the apatite component in GAp, played a significant role in strengthening the PLCL polymer matrix. The highest strength obtained in the nanocomposite was ~45 MPa, a value approximately four times higher than that of the pure PLCL (12 MPa). Recalling the morphology of the nanocomposite (shown in Figure 4), tiny apatite nanocrystallites were shown to be evenly distributed within the polymer matrix. Therefore, the fine inorganic crystallites distributed in the organic phase should provide the flexible matrix with high resistance to a plastic failure, improving the tensile strength significantly.[22] On the other hand, when the GAp content was relatively high, such a strengthening role of the inorganic apatite would be attenuated or negated because the apatite nanocrystallites were agglomerated (as observed in Figure 4) in which case the aggregated particles that were a few micrometers could act as a failure origin, resulting in the reduction of the overall strength of the matrix. In this sense, the use of GAp co-precipitates as the reinforcing phase of PLCL is considered to be highly effective in producing mechanically strong nanocomposites. Furthermore, the gelatin-driven apatite precipitation method should also be highlighted as it produces fine apatite crystals and allows for their even distribution throughout the nanocomposites.

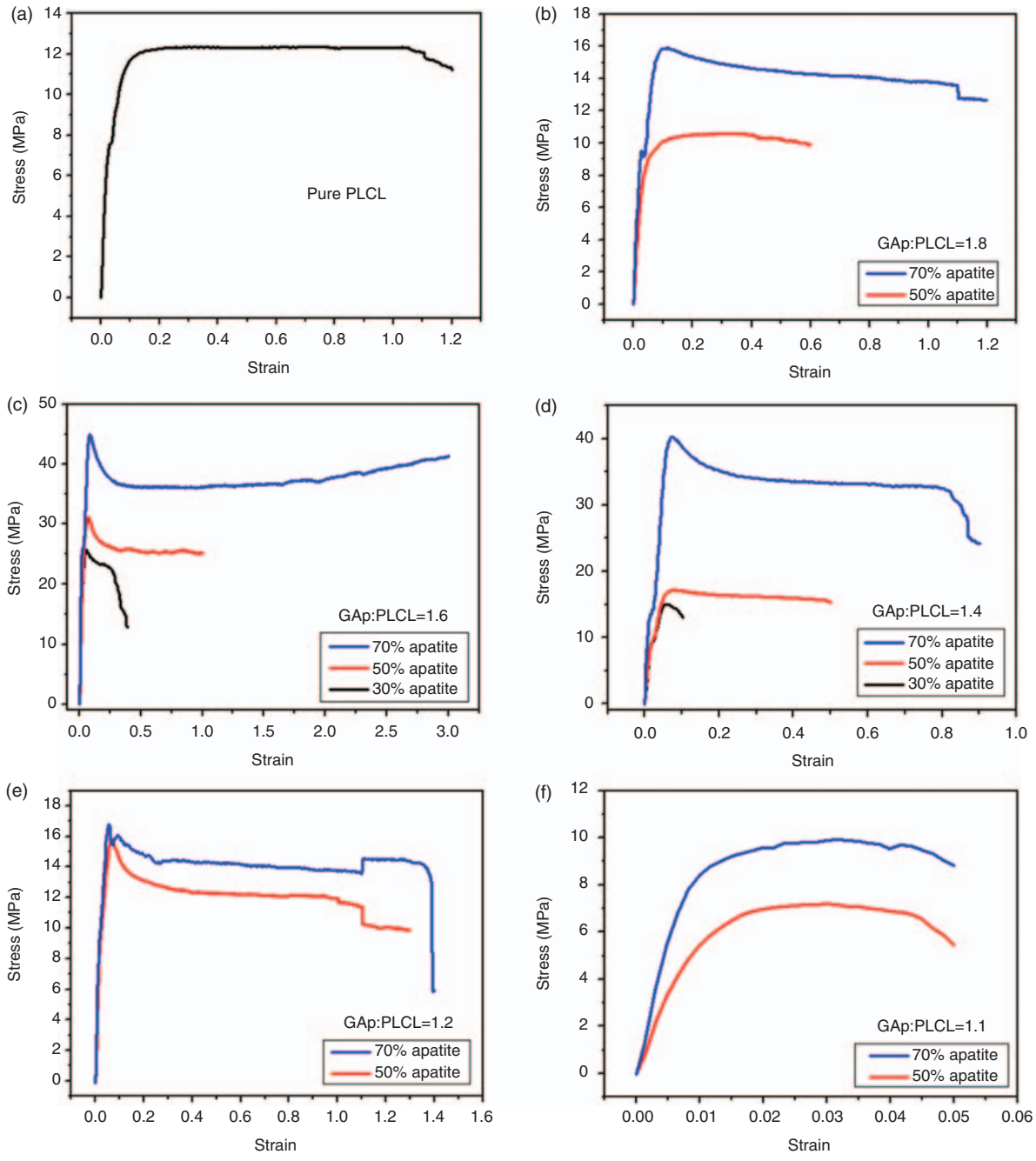

Figure 6. Stress–strain curves of the PLCL and GAp-PLCL nanocomposites with different compositions: (a) pure PLCL and (b–d) nanocomposites of GAp/PLCL 1:8 (b), 1:6 (c), 1:4 (d), 1:2 (e) and 1:1 (f). Note the different scales in *y*-axis to better show curve behaviors. Compared to PLCL, the nanocomposites resisted higher stresses prior to a yield point. In particular, tremendous improvements in stress resistance were observed with small contents of GAp (GAp/PLCL 1:6 and 1:4); moreover, such an improvement was more dominant when the apatite content was higher in GAp (70% >> 50% > 30% apatite).

The other mechanical properties of the nanocomposites, such as elastic modulus and elongation, were also observed. Figure 8 shows the elastic modulus of the nanocomposite with different compositions. A significant enhancement of the elastic modulus with the addition of GAp was only seen in the nanocomposite of GAp/PLCL 1:6. The increases in apatite content increased the elastic modulus, and the 70% apatite showed the maximum value (1500 MPa), representing a five-fold improvement (vs. 300 MPa in pure PLCL). With higher GAp content (GAp/PLCL 1:2, 1:4 and 1:8), there was no noticeable increase in the elastic modulus with respect to pure PLCL. The nanocomposites with the highest GAp content (GAp:PLCL = 1:1)

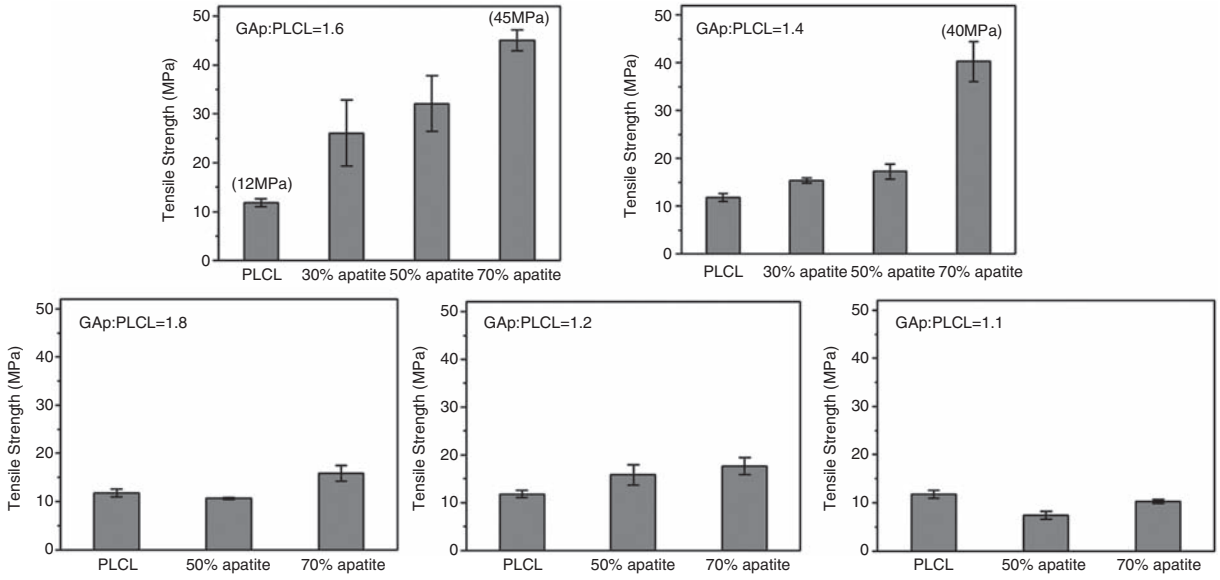

Figure 7. Tensile strength of the GAp-PLCL nanocomposites with different compositions. Data are presented at a fixed GAp/PLCL composition (1:6, 1:4, 1:8, 1:2 or 1:1) while varying the apatite content (30%, 50% and 70%). Pure PLCL was presented in each graph for comparison purposes.

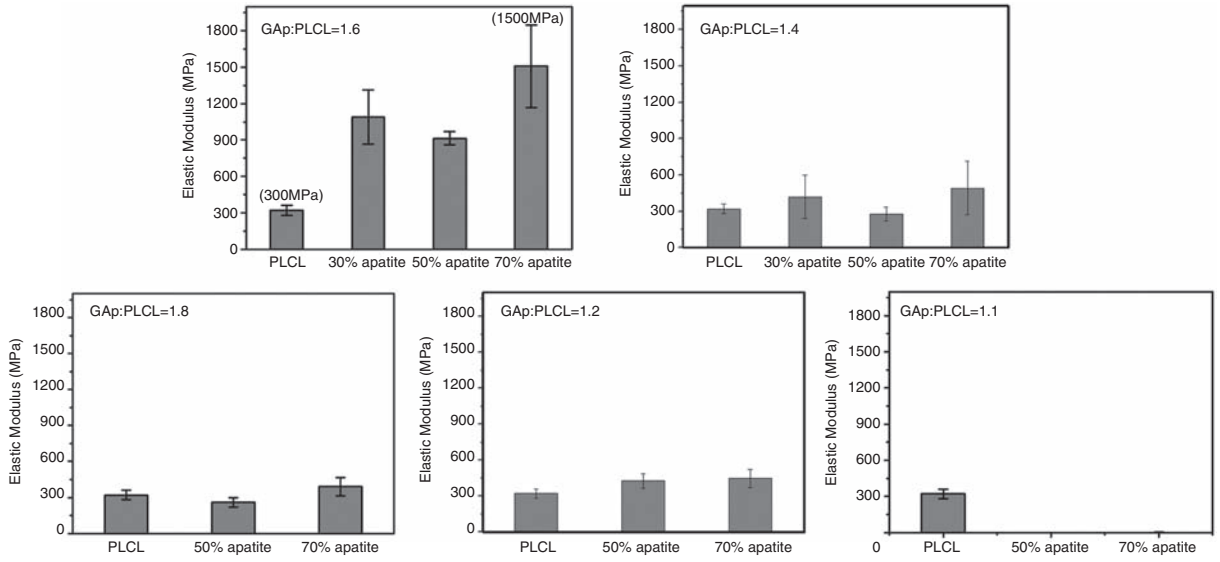

Figure 8. Elastic modulus of the GAp-PLCL nanocomposites with different compositions. Data are presented at a fixed GAp/PLCL composition (1:6, 1:4, 1:8. 1:2 or 1:1) while varying the apatite content (30%, 50% and 70%). Pure PLCL was presented in each graph for comparison purposes.

showed significantly reduced elastic modulus compared to pure PLCL. Similar to the tensile strength behaviors, the elastic modulus also showed significant improvement with the incorporation GAp at a proper content (GAp/PLCL 1:6) and in this GAp addition the apatite content was also helpful in enhancing the elastic modulus, demonstrating the effective roles of GAp in both strengthening and stiffening of the PLCL matrix.

The elongation behavior of the nanocomposite was also examined, by measuring the strain at failure, as shown in Figure 9. The elongation level of the nanocomposites was not substantially increased for all compositions, but for one composition (GAp/PLCL 1:6 with 70% apatite) there was a two-fold increase. In some nanocomposite compositions (particularly those with low apatite content and low GAp content) the

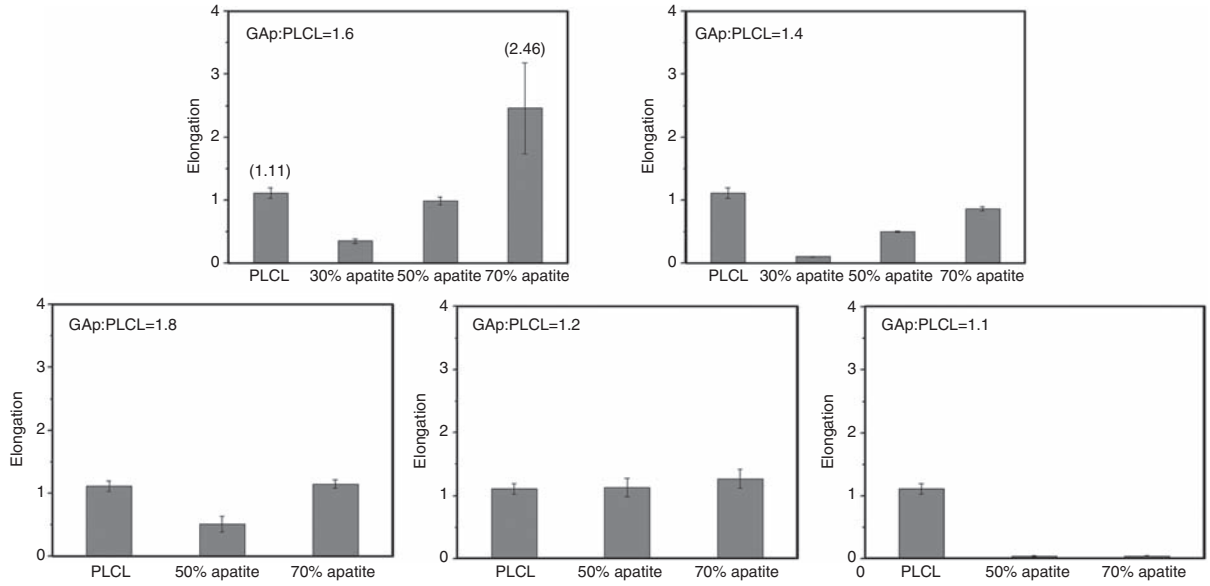

Figure 9. Elongation of the GAp-PLCL nanocomposites with different compositions. Data are presented at a fixed GAp/PLCL composition (1:6, 1:4, 1:8, 1:2 or 1:1) while varying the apatite content (30%, 50% and 70%). Pure PLCL was presented in each graph for comparison purposes.

elongation was even lowered with respect to that of pure PLCL. It is considered that GAp co-precipitates distributed within the PLCL matrix did not play a dominant role in sustaining the plastic deformation of polymeric chains as soon as the yield point (breakdown in elasticity) was reached. Although the GAp co-precipitates were well distributed within the polymer matrix, demonstrating effective resistance to elastic deformation and stress in this region, their role beyond the elastic region was not considered to be effective. One interesting point is that the increase in apatite content within GAp appeared to increase the elongation of nanocomposites (note the graphs in GAp/PLCL 6:1 and 4:1). This is considered to be related to the possible role of the apatite phase in increasing the alignment of polymeric chains during the plastic deformation, preventing the catastrophic failure of the randomly distributed polymeric chains.[17]

Conclusively, the GAp component added to PLCL matrix played significant roles in improving the mechanical properties, mainly the strength and elastic modulus, particularly when the GAp-PLCL nanocomposite was prepared with the proper composition, i.e. GAp/PLCL 1:6 with 70% apatite exhibited the optimal mechanical properties in terms of strength (four-fold improvement, 45 MPa vs. 12 MPa) and elastic modulus (five-fold improvement, 1500 MPa vs. 300 MPa). The GAp component was also effective in the elongation behavior at this specific composition, showing two-fold improvement compared to that of pure PLCL (2.46 vs. 1.11).

Apatite-forming ability and cellular responses of GAp-PLCL nanocomposites

Along with the mechanical properties, the biocompatibility of the GAp-PLCL nanocomposites was addressed. First, the in vitro apatite-forming ability of the nanocomposites in acellular conditions was examined by the SBF-immersion tests. For the biocompatibility tests we selected GAp/PLCL 1:6 as the representative composition, as it had proven to have optimal mechanical properties.

Figure 10 shows the surface morphology and chemistry change of the samples after the SBF-immersion tests. SEM morphology revealed that while no noticeable change was noticed in pure PLCL throughout the test period (Figure 10(a)), there was considerable formation of mineral phase on the surface of the nanocomposite (Figure 10(b)). The surface was almost completely covered with the mineralized crystals as early as 3 days. Some cracks were generated in the mineralized samples, which were possibly due to the thickened mineralized layer. The mineralized products in the nanocomposite were further characterized with XRD and ATR-FTIR. The XRD patterns showed the development of peaks (including a major peak at $2\theta = 32^{\circ}$), those related to apatite, after the SBF-immersion (Figure 10(c)). Although the apatite peaks were seen at a low intensity in the GAp-PLCL sample due to the presence of intrinsic apatite, the apatite peak intensities increased substantially after SBF-immersion, and the peak intensity increased with increasing

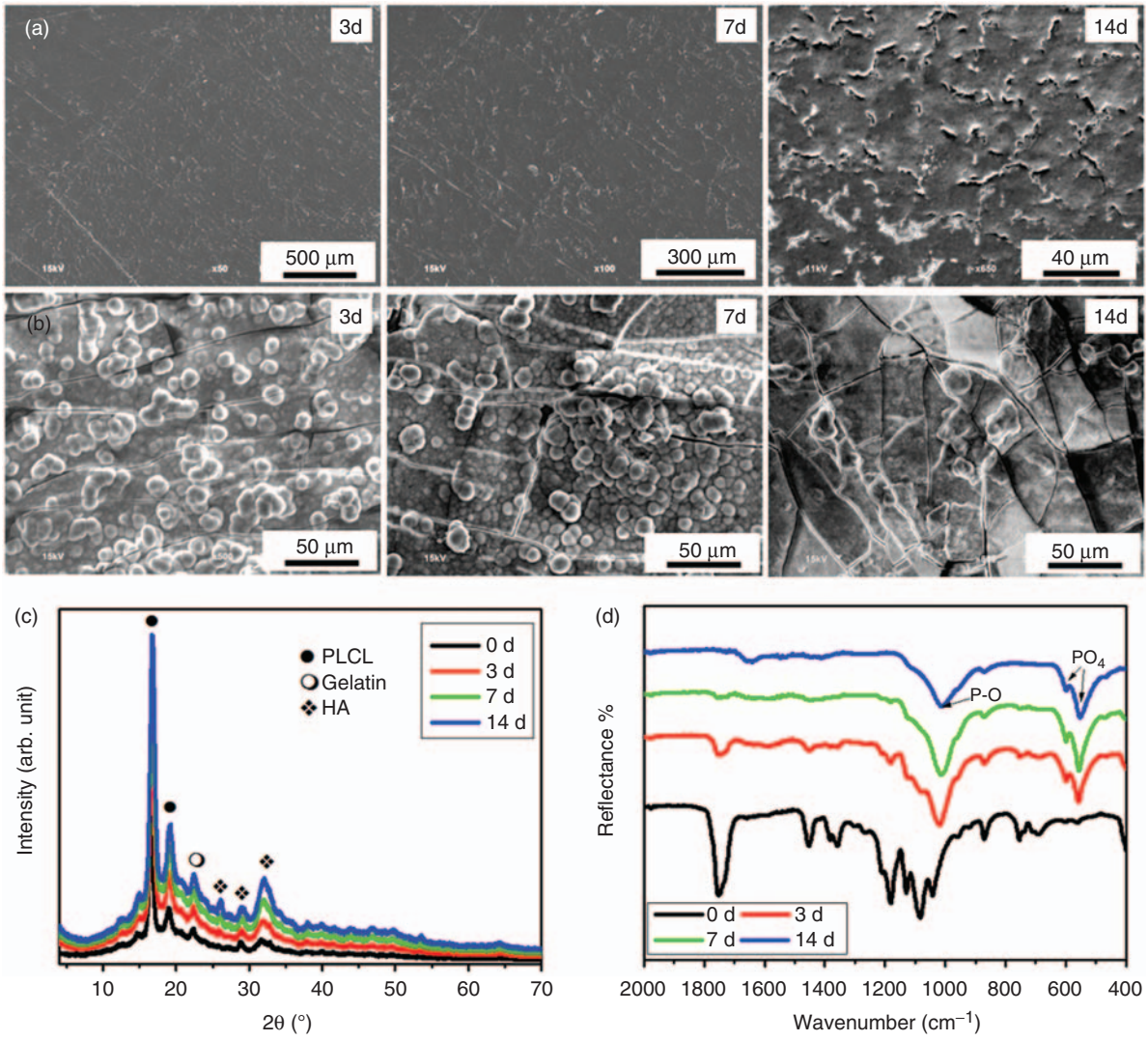

Figure 10. In vitro apatite forming ability of the samples (PLCL vs. GAp/PLCL 1:6) tested by immersion of each sample in SBF for different periods. SEM images of PLCL (a) and nanocomposite (b) at 3, 7 and 14 days, (c) XRD patterns and (d) ATR-FT-IR spectra of nanocomposite sample at different SBF-immersion periods.

immersion time. The ATR-FTIR spectra of the nanocomposite samples revealed chemical bands associated with apatite, i.e. 1000–1100 cm^{-1} (P–OH bending in HPO_4), 450–650 cm^{-1} (P–O stretching in HPO_4), and 1000–1100 cm^{-1} (P–O stretching in PO_4) (Figure 10(d)). As the immersion time increased, those band intensities increased correspondingly. The results demonstrated the effective role of the GAp co-precipitate component within the PLCL matrix in inducing apatite mineral phase formation on the surface. It is concluded that both the gelatin and apatite phase present in the GAp co-precipitates should improve the mineralization. The gelatin phase, consisting of a collection of amino acid sequences, will attract calcium ions and the accompanying deposition of phosphate ions to induce CaP mineralization.[26,27] The increased hydrophilic nature of the surface of the GAp-PLCL nanocomposite would enhance the ionic interactions and their surface deposits. It is also possible that the intrinsic apatite phase would provide calcium and phosphate ionic sources for the supersaturation of SBF, and consequent calcium phosphate re-precipitation.[28] This rapid apatite mineral formation allows one to consider the nanocomposite surface as a favorable and effective substrate for cells to adhere to and to develop into an osteogenic lineage.[29–31]

We next cultured cells onto the nanocomposite and investigated the cellular behaviors, including the proliferation and osteogenic differentiation. MC3T3-E1 preosteoblastic cells were plated onto either PLCL or nanocomposite samples, and were then cultured in an osteogenic medium for up to 14 days. First, cell proliferation behavior was examined by measuring cell viability at each culture period (Figure 11(a)). At day 1,

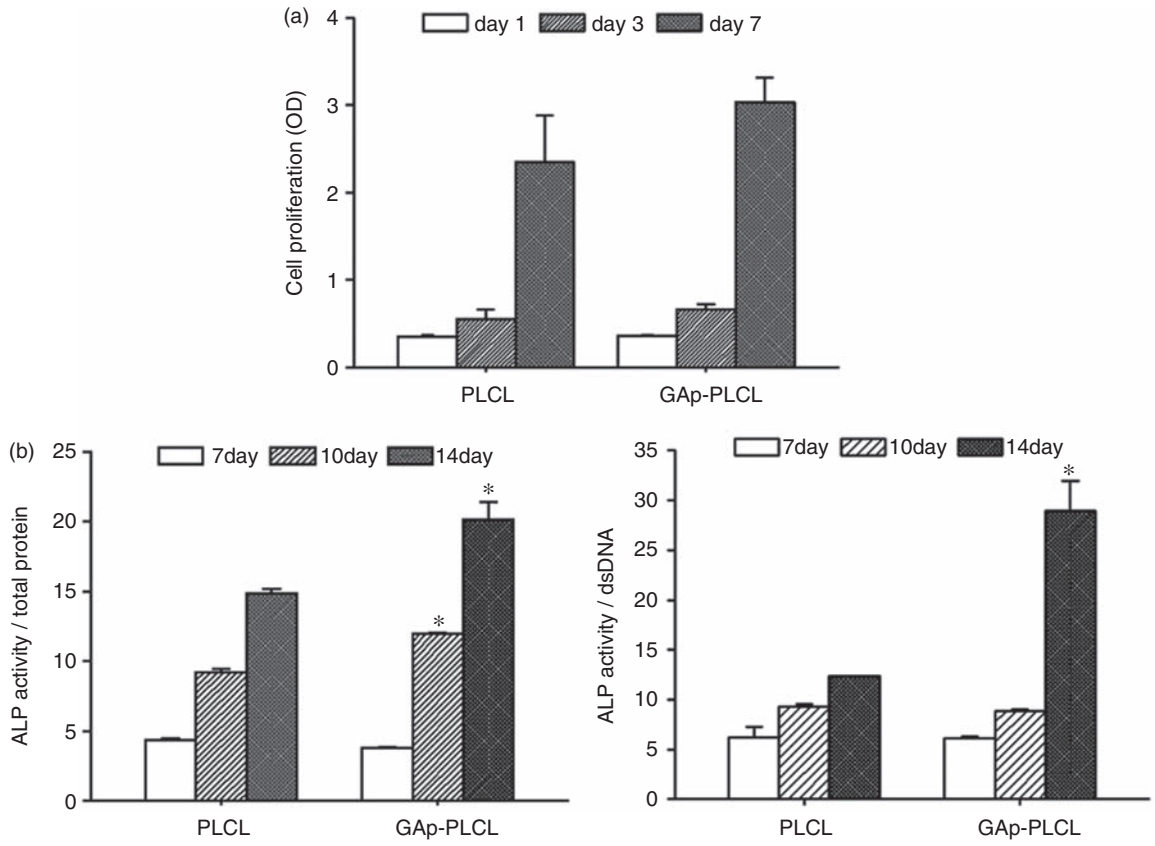

Figure 11. Biocompatibility of the GAp-PLCL nanocomposite samples, as assessed by the in vitro cell proliferation and osteogenic differentiation; (a) cell proliferation on the samples (PLCL vs. GAp/PLCL 1:6) compared for up to 7 days, showing an on-going increase with culture time, suggesting good cell viability, and (b) ALP activity of cells on the samples at days 7, 10 and 14. ALP activity levels are represented when normalized either to total protein content or to total dsDNA content. A statistically significant difference was noticed, $*p < 0.05$.

the cell viability level was comparable for both sample groups. Cell proliferation increased with culture time, with a particularly high increase observed at day 7, and the increase appeared to be higher in the nanocomposite, which however, did not show any statistical significance ($p > 0.05$).

The osteogenic differentiation of the cells was evaluated by means of determining ALP activity. ALP is known as an important early-stage marker for osteogenic differentiation of many cells, including MC3T3-E1 pre-osteoblasts.[32,33] The ALP enzymatic activity was measured at 7, 10 and 14 days, and the level was presented after normalizing either to total protein or total dsDNA (Figure 11(b)). The ALP activity levels of cells grown on both sample groups were similar at day 7. However, after culturing for 10 and 14 days, cells on the nanocomposite expressed significantly higher ALP activity than those grown on PLCL, for both normalized cases. When normalized to total dsDNA content, particularly at 14 days, the ALP difference between PLCL and nanocomposite was higher. While the cell proliferation on both sample groups was similarly observed, the osteogenic differentiation, as assessed by the ALP activity, was demonstrated to be significantly higher on the nanocomposite. Moreover, the ALP stimulation was more noticeable as the culture period increased, signifying that the efficacy of the GAp added to PLCL was elicited at the osteoblastic differentiation stage of MC3T3-E1 cells. More in-depth experiments, including the identification of other differentiation markers, and the confirmation of cellular mineralization are considered as future studies, to substantiate the osteogenic stimulatory role of the GAp component. Moreover, the GAp component will also be introduced to other types of biopolymers to find extended applications.

Conclusions

Bone-targeting nanocomposites were developed by combining PLCL and GAp bone mimetic components derived from a co-precipitation reaction. The incorporation of GAp co-precipitates into the PLCL matrix significantly increased the hydrophilicity, acellular

mineralization behavior, and the osteogenic differentiation of cells. The mechanical properties of the GAp-PLCL nanocomposites were enormously improved, including tensile strength and elastic modulus, as high as four/five-fold, and elongation was increased about two-fold, each with respect to the properties of pure PLCL. This was exclusively possible when the added GAp content was low enough to develop a well-dispersed GAp component, without being agglomerated within the PLCL matrix. The mechanical and biological properties of the GAp-PLCL nanocomposites observed in this study hold great promise for their uses as bone regenerative matrices.

Conflict of interest

None declared.

Funding

This study was supported by grant from Priority Research Centers Program (2009-0093829), National Research Foundation, South Korea.

References

1. Hu Y, Zhang C, Zhang S, et al. Development of a porous poly(L-lactic acid)/hydroxyapatite/collagen scaffold as a BMP delivery system and its use in healing canine segmental bone defect. *J Biomed Mater Res Part A* 2003; 67: 591–598.
2. Fujihara K, Kotaki M and Ramakrishna S. Guided bone regeneration membrane made of polycaprolactone/calcium carbonate composite nano-fibers. *Biomaterials* 2005; 26: 4139–4147.
3. Kim HW, Lee HH and Knowles JC. Electrospinning biomedical nanocomposite fibers of hydroxyapatite/poly(lactic acid) for bone regeneration. *J Biomed Mater Res Part A* 2006; 79: 643–649.
4. Song JH, Kim HE and Kim HW. Electrospun fibrous web of collagen–apatite precipitated nanocomposite for bone regeneration. *J Mater Sci Mater Med* 2008; 19: 2925–2932.
5. Venugopal J, Vadgama P, Sampath Kumar TS, et al. Biocomposite nanofibres and osteoblasts for bone tissue engineering. *Nanotechnology* 2007; 18: 1–8.
6. Liao S, Wang W, Uo M, et al. A three-layered nano-carbonated hydroxyapatite/collagen/PLGA composite membrane for guided tissue regeneration. *Biomaterials* 2005; 26: 7564–7571.
7. Jang JH, Oscar C and Kim HW. Electrospun materials as potential platforms for bone tissue engineering. *Adv Drug Deliv Rev* 2009; 61: 1065–1083.
8. Marouf HA, Quayle AA and Sloan P. In vitro and in vivo studies with collagen/hydroxyapatite implants. *Int J Oral Maxillofac Implants* 1990; 5: 148–154.
9. Hong SJ, Yu HS, Noh KT, et al. Novel scaffolds of collagen with bioactive nanofiller for the osteogenic stimulation of bone marrow stromal cells. *J Biomater Appl* 2010; 24: 733–750.
10. Song JH, Kim HE and Kim HW. Collagen-apatite nanocomposite membranes for guided bone regeneration. *J Biomed Mater Res Part B Appl Biomater* 2007; 83: 248–257.
11. Kim HW, Lee HH and Chun GS. Bioactivity and osteoblast responses of novel biomedical nanocomposites of bioactive glass nanofiber filled poly(lactic acid). *J Biomed Mater Res Part A* 2008; 85: 651–663.
12. Erisken C, Kalyon DM and Wang H. Functionally graded electrospun polycaprolactone and β-tricalcium phosphate nanocomposites for tissue engineering applications. *Biomaterials* 2008; 29: 4065–4073.
13. Kim HW, Song JH and Kim HE. Nanofiber generation of gelatin-hydroxyapatite biomimetics for guided tissue regeneration. *Adv Funct Mater* 2005; 15: 1988–1994.
14. Kim HW, Kim HE and Salih V. Stimulation of osteoblast responses to biomimetic nanocomposites of gelatin-hydroxyapatite for tissue engineering scaffolds. *Biomaterials* 2005; 26: 5221–5230.
15. Jell G and Stevens MM. Gene activation by bioactive glasses. *J Mater Sci Mater Med* 2006; 17: 997–1002.
16. Lee HH, Yu HS, Jang JH, et al. Bioactivity improvement of poly(ε-caprolactone) membrane with the addition of nanofibrous bioactive glass. *Acta Biomater* 2008; 4: 622–629.
17. Li Z, Zhao X, Ye L, et al. Structure and blood compatibility of highly oriented PLA/MWNTs composites produced by solid hot drawing. *J Biomater Appl*. Epub ahead of print 2 June 2013. doi: 10.1177/0885328213490047.
18. Dorj B, Won JE, Kim JH, et al. Robocasting nanocomposite scaffolds of poly(caprolactone)/hydroxyapatite incorporating modified carbon nanotubes for hard tissue reconstruction. *J Biomed Mater Res Part A* 2013; 101: 1670–1681.
19. Shin US, Yoon IK, Lee GS, et al. Carbon nanotubes in nanocomposites and hybrids with hydroxyapatite for bone replacements. *J Tissue Eng* 2011; 2: 674287.
20. Lahiri D, Rouzaud F, Richard T, et al. Boron nitride nanotube reinforced polylactide–polycaprolactone copolymer composite: mechanical properties and cytocompatibility with osteoblasts and macrophages in vitro. *Acta Biomater* 2010; 6: 3524–3533.
21. Perez RA, Kim HW and Ginebra MP. Polymeric additives to enhance the functional properties of calcium phosphate cements. *J Tissue Eng* 2012; 3: 20417314 12439555.
22. Mammeri F, Bourhis EL, Rozesa L, et al. Mechanical properties of hybrid organic–inorganic materials. *J Mater Chem* 2005; 15: 3787–3811.
23. Jegal SH, Park JH, Kim JH, et al. Functional composite nanofibers of poly(lactide–co-caprolactone) containing gelatin–apatite bone mimetic precipitate for bone regeneration. *Acta Biomater* 2011; 7: 1609–1617.
24. Minna H and Ann-Christine A. Heterogeneous biodegradation of polycaprolactone–low molecular weight products and surface changes. *Macromol Chem Phys* 2002; 203: 1357–1363.
25. Dorgan JR, Braun B, Wegner JR, et al. Poly(lactic acids): a brief review. *ACS Symp Ser* 2006; 939: 102–125.

26. Teng S, Shi J and Chen L. Formation of calcium phosphates in gelatin with a novel diffusion system. *Colloid Surf B: Biointerf* 2006; 49: 87–92.
27. Chang MC and DeLong R. Calcium phosphate formation in gelatin matrix using free ion precursors of Ca^{2+} and phosphate ions. *Dent Mater* 2009; 25: 261–268.
28. Jalota S, Bhaduri SB and Tas AC. Osteoblast proliferation on neat and apatite-like calcium phosphate-coated titanium foam scaffolds. *Mater Sci Eng C* 2007; 27: 432–440.
29. Kim JJ, Jin GZ, Yu HS, et al. Providing osteogenesis conditions to mesenchymal stem cells using bioactive nanocomposite bone scaffolds. *Mater Sci Eng C* 2012; 32: 2545–2551.
30. Khanna-Jain R, Mannerstrom B, Vuorinen A, et al. Osteogenic differentiation of human dental pulp stem cells on β-tricalcium phosphate/poly (l-lactic acid/caprolactone) three-dimensional scaffolds. *J Tissue Eng* 2012; 3: 2041731412467998.
31. He W, Andersson M, de Souza PP, et al. Osteogenesis-inducing calcium phosphate nanoparticle precursors applied to titanium surfaces. *Biomed Mater* 2013; 8: 035007.
32. Yu HS, Hong SJ and Kim HW. Surface-mineralized polymeric nanofiber for the population and osteogenic stimulation of rat bone-marrow stromal cells. *Mater Chem Phys* 2009; 113: 873–877.
33. McComb RB, Bowers Jr GN and Posen S. *Alkaline phosphatase*. New York, NY: Plenum, 1979.